Annals of the Academy of Romanian Scientists
Edition ONLINE Physics Series
ISSN 2066-8589 Volume **1**, Number **2**/**2009**

ASSESSMENTS OF DELAYED HYDRIDE CRACKING PHENOMENON FOR THE FUEL PRESSURE TUBE OF THE CERNAVODĂ NUCLEAR POWER PLANT

S. FLOREA[1], V. RADU[1], V. IONESCU[1], M. PAVELESCU[2]

Abstract. *A critical review of the DHC (Delayed Hydride Cracking) phenomenon in the specific case of the pressure tube subcomponent of the fuel channel assembly of the Cernavodă Nuclear Power Plant is presented. For the both stages of DHC –initiation and propagation- the models are discussed and an appropriate numerical assessment was implemented into CANTUP computer code. A first task of the present work is to couple the routines for DHC initiation and propagation steps for better modeling of the characteristics of this damaging phenomenon. Finally, the assessment of DHC rates in the case of various locations of the virtual crack on the CANDU pressure tube is performed. The normal operation conditions for ten years period of time are assumed to consider their influence on the material properties.*

Keywords: Key words: crack propagation velocity, stress intensity factor, hydride platelet, embrittlement, Zr-2.5% Nb alloy

1. Introduction

Zirconium alloys are used in the water reactors because of their low capture cross-section for thermal neutrons and good mechanical and corrosion properties. Unfortunately, hydrogen was identified as an embrittlement agent, as, on reasons of solubility in the alloy matrix, it precipitates as hydride platelets [1]. Many experimental results [2] pointed out that Zr-2.5% Nb alloys may also fracture by a time-dependent mechanism involving hydrogen, but the first practical confirmation of such a mechanism was the cracking of experimental fuel cladding made from Zr-2.5 % Nb. Hydrides were associated with the cracks and the process was called Delayed Hydride Cracking – abbreviated DHC [3].

In order to describe in a quantitative way this phenomenon it is necessary to evaluate the stress-strain field of the specimen which contain the crack susceptible to extent by DHC; this concern either initiation and propagation. Usually, this is done using finite element method and certain calculus programs/codes. In the case of the Institute of Nuclear Research from Pitesti (INR), for the fuel channel assembly, it was developed over the time a code, called CANTUP. The CANTUP

[1]Str. Câmpului, Nr. 1, POB 78, Postal Code 115400 - Mioveni, Argeș County, Romania (e-mail: silviu.florea@nuclear.ro).
[2]Academy of Romanian Scientists, 54, Splaiul Independenței, Sector 5, 050094 Bucharest, Romania.

code is software for thermomechanical analysis in the case of two-dimensional plane or three-dimensional axis symmetric structure. It is used at INR Pitești for long term behavior evaluation of the fuel channel assembly by means of the equivalent bars approximation [4]. The code contains an original creep law, experimentally obtained at INR Pitești which includes the irradiation induced creep. Also, the code is able to analyze the simulation the pressure tube – spacers – calandria tube contact. This code has been developed to perform also probabilistic analysis [5], [6].

Delayed hydride cracking is a sub-critical crack growth mechanism occurring in zirconium alloys as well as other hydride-forming materials that requires the formation of brittle hydride phases at the tip of a crack and subsequent failure of that hydride resulting in crack extension, as is depicted in Figure 1.

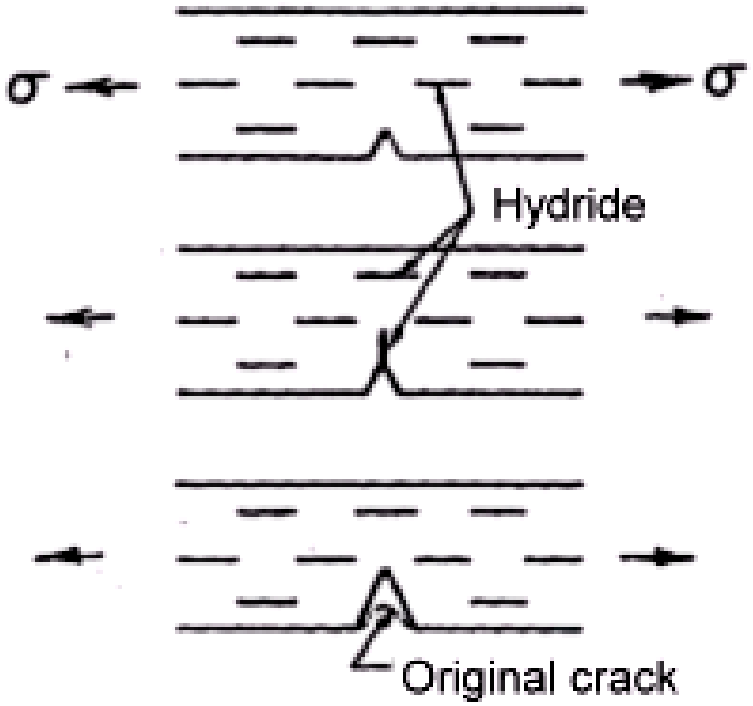

Fig. 1. A schematic illustration of a single step in DHC starting with a notch under stress(top), hydride precipitation at the notch (middle) and fracture of hydride and crack extension from the notch (bottom).

Similar with many other stable crack propagation mechanisms, the phenomenon of DHC can be generally described by the dependence of the crack growth rate or crack velocity on the applied stress intensity factor. The general shape of such a relationship is illustrated in Figure 2 [7]. This figure shows that, at stress intensities below a threshold, K_{IH}, cracks do not grow even though a quantity of hydride may accumulate at a crack tip under stress.

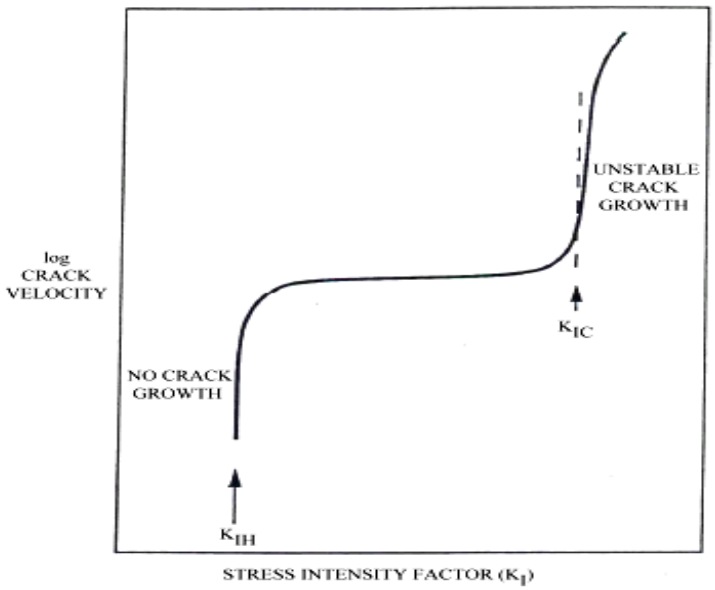

Fig. 2. A schematic representation of the relationship between crack velocity and stress intensity factor for the DHC phenomenon.

2. Threshold Stress Intensity Factor Kih for Delayed Hydride Crack Propagation

The model used in the present work has been described in [8] and introduces the concept of process zone, whose main features are displayed depicted in Figure 3.

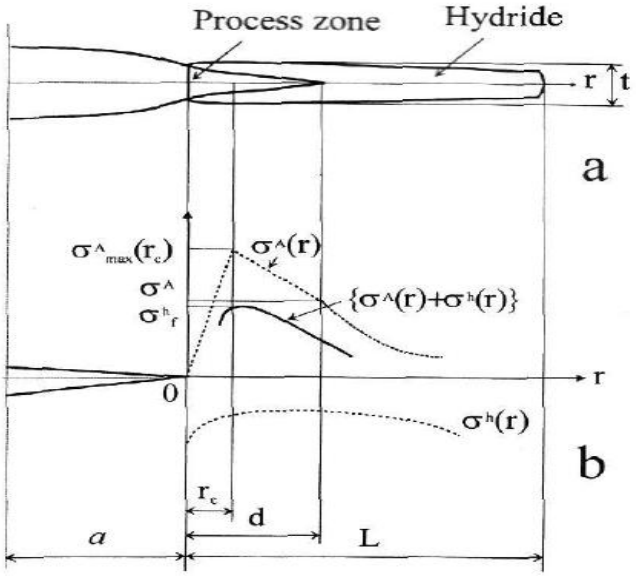

Fig. 3: Process zone model **a)** the hydride platelet of length *L* covering the process zone of length d. **b)** the local stress distribution within the process zone.

Here the meanings of the parameters are: d is the process zone length; L is the length of the hydride covering the process zone; σ_h is the compressive stress due to the hydride formation as a consequence of a larger volume of the hydride compared with the zirconium alloy matrix; σ^A is the applied remote stress (tensile); r_c is the critical distance in the front of the crack tip, where the applied stress reaches its maximum; r is the distance in front of the crack tip; a is the crack length.

The fracture condition is given by:

$$\sigma_{\max}^{\mathrm{A}}(\mathrm{r_c}) + \sigma^{\mathrm{h}}(\mathrm{r_c}) = \sigma_{\mathrm{f}}^{\mathrm{h}} \tag{1}$$

where σ_f^h is the critical stress to initiate fracture inside of the hydride.

The model assumes that the crack extends virtually from the actual crack-tip $x=a$ by the cohesive zone length d according to the Dugdale-Barenblatt [8] type cohesive zone, in order to avoid singularity of the stress near the crack tip. The length of the cohesive zone is considered equal with that of the process zone. The cohesive zone model is represented in Figure 4 [8]

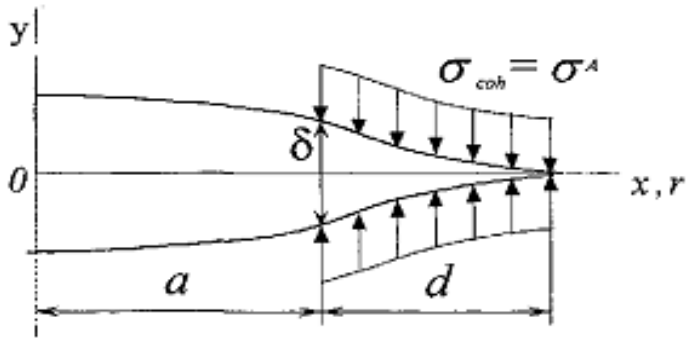

Fig. 4. The cohesive zone model ahead of the crack tip.

where: δ is the crack tip opening displacement σ_{coh} is the cohesive stress which acts over the crack surfaces. Between r_C and d it can be proved that exist the following relationship:

$$\mathrm{r_c} = \mathrm{k} \cdot \mathrm{d} \tag{2}$$

where k is a coefficient which depend on the approximation used. For the plane stress case the model use:

$$\mathrm{k} = \frac{\mathrm{E}' \cdot \left(\dfrac{4 \cdot \mathrm{K_I^2} \cdot (1 - 2 \cdot \nu) \cdot (1 - \nu^2)}{\mathrm{E} \cdot \pi \cdot \mathrm{t} \cdot \sigma_y} - \dfrac{(1 - \nu^2) \cdot \sigma_y}{\mathrm{E}} \right)}{\sigma_y} \tag{3}$$

where E is modulus of elasticity, t is the hydride thickness, E' is modulus of elasticity in linear plastic domain, ν is Poisson coefficient, K_I is first mode (opening-mode) [9] stress intensity factor, σ_y is yield stress. The value of K_I for which equation [1], after successive replacements, is satisfied is noted K_{IH} and it is called threshold value.

The model gives solution for the stress intensity threshold value K_{IH} in both plane stress and plane strain approximations of the stress-strain three dimensional field. Subsequently, it is introduced the mixed-mode approximation of the triaxial stress field, as a combination of plane stress and plane strain states, and the stress intensity value for this new case is:

$$\mathrm{K}_{\mathrm{IH}}^2 = \frac{\mathrm{E}\cdot\mathrm{t}\cdot\varepsilon_{\perp}\cdot\sigma_y^2}{2\cdot\mathrm{k}\cdot\left(1-\nu^2\right)\cdot\left(\dfrac{\sigma_y+\mathrm{k}\cdot\sigma_y}{1-2\cdot\nu}-\sigma_f^h\right)} \tag{4}$$

where $\varepsilon_{\perp}$ is the misfit strain due to the increased volume of the hydride volume, and for k is used the expression for plane stress value (3). Equation (4) is transcendent: k depends on K_I, i.e K_{IH}.

In order to perform numerical evaluations the following relationships are used [10]:

$$\mathrm{E} = 95900 - 57.4\cdot(\mathrm{T}-273)(\mathrm{MPa});\ \nu = 0.436 - 4.8\cdot10^{-4}\cdot(\mathrm{T}-300)$$

$$\sigma_y = 1088 - 1.02\cdot\mathrm{T}(\mathrm{MPa});\quad \sigma_f^h = 7.357\cdot10^{-3}\cdot\mathrm{E};\quad \mathrm{E}' = \mathrm{E}\cdot0.01 \tag{5}$$

where T is the temperature in °K,

The hydride thickness, t, produced at the crack tip subject to DHC phenomenon, has been considered temperature dependent. For the plane stress approximation the expression, also use in the mixed-mode approximation, is:

$$\mathrm{t} = 5.493 - 2.3\cdot10^{-2}\cdot\mathrm{T} + 5.7\cdot10^{-5}\cdot\mathrm{T}^2(\mu\mathrm{m}) \tag{6}$$

3. The Assessment of the Crack Propagation

The main assumptions of the models [11], [12] for the crack velocity assessment are presented in Figure 5.

The expression obtained for DHC velocity is

$$\mathrm{v} = \frac{2\cdot\pi\cdot\mathrm{D_H}}{\Omega_{Zr}\cdot\ln(\mathrm{L})\cdot\mathrm{l}\cdot\mathrm{t}\cdot\mathrm{N_H}\cdot\mathrm{x_{stoech}}}\cdot\left(\mathrm{C_{heat}^H}\cdot\mathrm{e}^{\dfrac{\mathrm{w_t^a(L)}}{\mathrm{R}\cdot\mathrm{T}}} - \mathrm{C_{cool}^H}\cdot\mathrm{e}^{\dfrac{\mathrm{w_t^a(l)}}{\mathrm{R}\cdot\mathrm{T}}}\right) \tag{7}$$

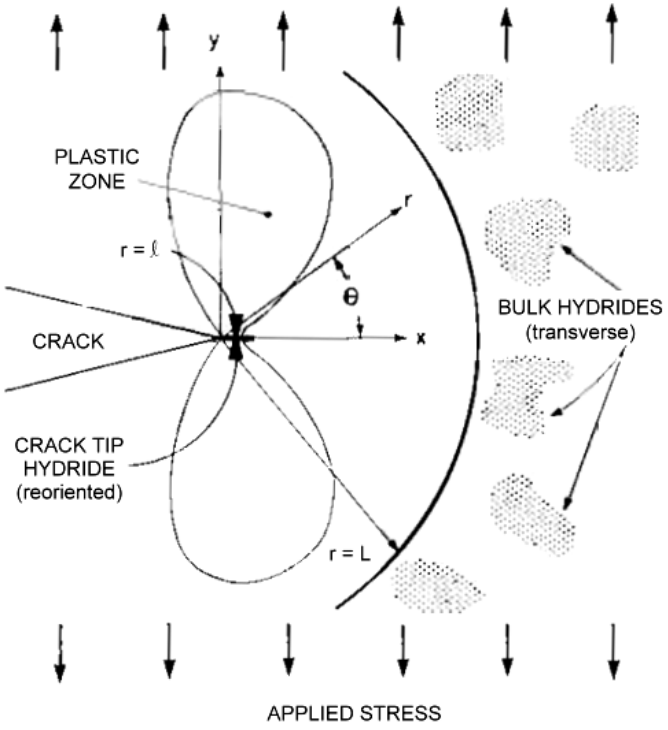

Fig. 5. The main assumptions for DHC modelling.

where, l and L are illustrated in Figure 5, and represent the plastic zone radius from the crack tip, respectively average distance between hydrides inside the matrix alloy, considered to be in an elastic tension state. It also have the average diffusion distance, within the alloy matrix, for hydrogen atoms which precipitates as hydride platelet formed at the crack tip. The other parameters for Equation (7) are: C_{heat}^{H} and C_{cool}^{H} are the limits of solubility of the hydrogen dissolved in the Zr matrix, in the hydrides presence, which reaches this state after a dissolution, respectively a growth process, D_H is the diffusion coefficient of for H in Zr, W_{Zr} represents Zr atomic volume, t the thickness of the hydride in front of the crack tip, N_H the atomic hydride density, x_{stoech} is the number of the atoms in ZrH_x.

The parameters C_{heat}^{H} and C_{cool}^{H} are correlated with the following relationship:

$$C_{cool}^{H} = C_{heat}^{H} \cdot e^{\frac{(Q_{cool} - Q_{heat})}{RT}} \tag{8}$$

where Q_{heat} and Q_{cool} represent the activation energy for dissolution respectively for growth of hydrides in Zr alloys. The $w_t^a(L)$ and $w_t^a(l)$ quantities are the interaction energies per H mol due to the formation of hydrides at L and l distances (Figure 5),

$$w_t^a = -V_{hidr} \cdot \sigma_{ij} \cdot e_{ij} \tag{9}$$

where V_{hidr} is the volume per H mole, σ_{ij} applied stress, e_{ij} accommodation strain (stress free), with repeated summation after *i* and *j*.

At *l* distance (Figure 5) the stresses are:

$$\sigma_{11} = 2.08 \cdot \sigma_y; \quad \sigma_{22} = 3.35 \cdot \sigma_y; \quad \sigma_{33} = 2.71 \cdot \sigma_y \tag{10}$$

while at *L* distance (Figure 5):

$$\sigma_{11} = \sigma_{22} = -\frac{K_I}{\sqrt{2 \cdot \pi \cdot L}}; \quad \sigma_{33} = \nu \cdot (\sigma_{11} + \sigma_{22}) \tag{11}$$

l is evaluated with:

$$l = 2 \cdot \delta = 2 \cdot \frac{0.8 \cdot (1 - \nu^2) \cdot K_I}{E \cdot \sigma_y} \tag{12}$$

where δ is the well-known crack tip opening displacement (CTOD).

L is considered to be depending on stress intensity factor:

$$L = \frac{L^0 \cdot K_I^2}{(K_I^0)^2} \quad \left(L^0 = 340\mu m; K_I^0 = 6 \cdot MPa \cdot \sqrt{m}\right) \tag{13}$$

In order to perform numerical calculus, it has been used the dependencies [10] given by the Equations set (14):

$$D_H = 2.17 \cdot 10^{-7} \cdot \mathbf{e}^{\frac{-35.100 \frac{kJ}{mol}}{R \cdot T}} \left(\frac{m^2}{s}\right); \quad \Omega_H = 2.3 \cdot 10^{-29} (m^3)$$

$$N_H = 6.13 \cdot 10^{28} \quad \left(\frac{atomi}{m^3}\right); \quad t = 2.5(\mu m); \quad e_{11} = e_{22} = 0.458; \quad e_{33} = 0.072$$

$$C_{heat}^H = 10.32 \cdot \mathbf{e}^{\frac{-35.578 \frac{kJ}{mol}}{R \cdot T}} \left(\frac{atom}{atom}\right); \quad V_H = 16.7 \cdot 10^{-7} \left(\frac{m^3}{mol\ H}\right)$$

$$V_{hydr} = 16.3 \cdot 10^{-6} \left(\frac{m^3}{mol\ hidrură}\right); \tag{14}$$

4. The Coupling of the DHC Modeling and CANTUP Code

The coupling between CATUP code and the modeling related on initiation and propagation of the DHC phenomenon consists in the transfer of the data related on the stress-strain state obtained with the FEM method, by means of the CANTUP code, to the DHC models. The stress-strain state is reflected in the K_I parameter. This parameter is contained in the crack velocity formulae, and also, by comparing with the threshold value corresponding to the local temperature, it decides if the propagation of the crack in the brittle material (i.e. the hydride in front of the crack tip) starts or not. The coupling logical flowchart is represented in Figure 6.

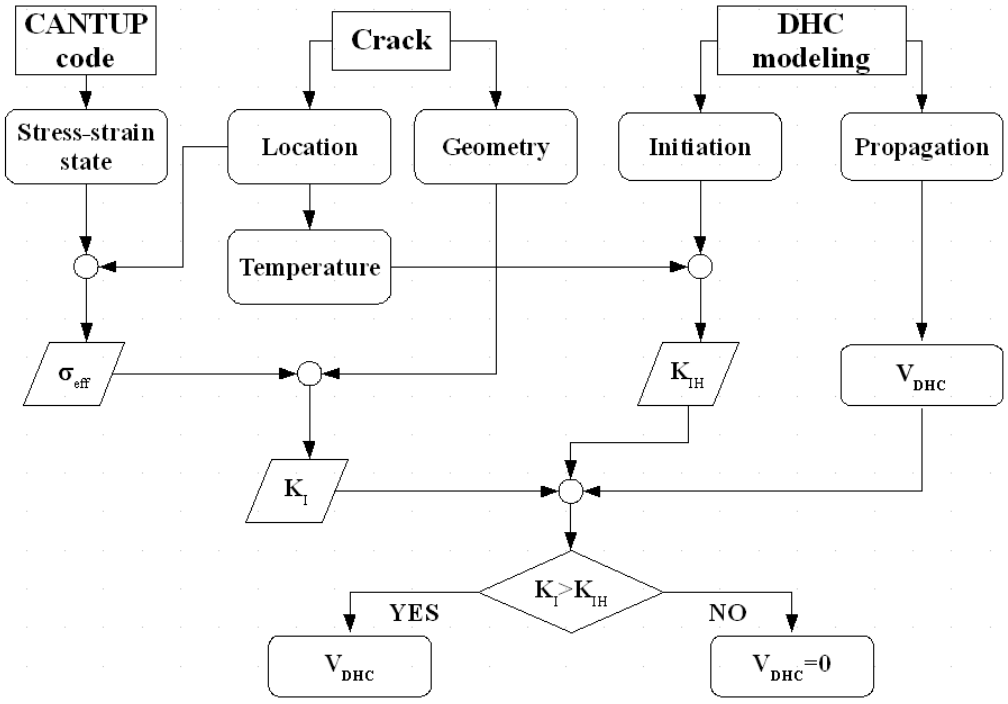

Fig. 6. Flowchart of the DHC modeling and CANTUP code coupling.

The evaluation of the stress intensity factor have been performed with a known scheme (see Figure 7, ref [13]), corresponding to the approximation of a semi elliptical surface flaw in a plate.

For membrane tensile stress, σ_m, it have been used the equivalent stress obtained on the elements of the lower face of the pressure tube equivalent bar. On these elements the greatest values of the stress have been obtained, because the pressure tube – spacers – calandria tube contact. σ_b was considered null. Dimensions $2W$ and t have been taken the width and the thickness of the pressure tube equivalent bar (ref. [4]), respectively. For a and $2c$ values 1.5 mm and 4 mm have been used [14].

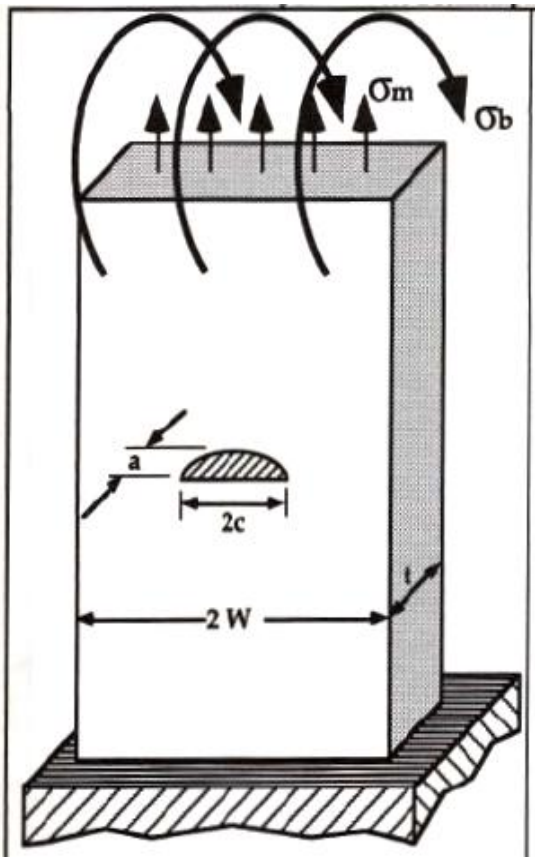

σ_m - Membrane (tensile) stress.
σ_b - Bending stress

$$\sigma_b = \frac{Mt}{2I}$$

where

$$I = \frac{Wt^3}{6}$$

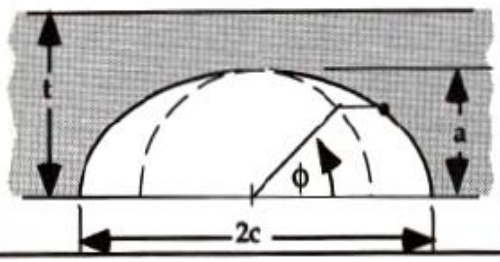

$$K_I = (\sigma_m + H\sigma_b)\sqrt{\frac{\pi a}{Q}}F\left(\frac{a}{t},\frac{a}{c},\frac{c}{W},\phi\right)$$

where

$$Q = 1 + 1.464\left(\frac{a}{c}\right)^{1.65}$$

$$F = \left[M_1 + M_2\left(\frac{a}{t}\right)^2 + M_3\left(\frac{a}{t}\right)^4\right] f_\phi f_w g$$

$$M_1 = 1.13 - 0.09\left(\frac{a}{c}\right)$$

$$M_2 = -0.54 + \frac{0.89}{0.2 + \frac{a}{c}}$$

$$M_3 = 0.5 - \frac{1.0}{0.65 + \frac{a}{c}} + 14\left(1.0 - \frac{a}{c}\right)^{24}$$

$$f_\phi = \left[\left(\frac{a}{c}\right)^2 \cos^2\phi + \sin^2\phi\right]^{1/4}$$

$$f_w = \left[\sec\left(\frac{\pi c}{2W}\sqrt{\frac{a}{t}}\right)\right]^{1/2}$$

$$g = 1 + \left[0.1 + 0.35\left(\frac{a}{t}\right)^2\right](1 - \sin\phi)^2$$

$$H = H_1 + (H_2 - H_1)(\sin\phi)^p$$

$$p = 0.2 + \frac{a}{c} + 0.6\left(\frac{a}{t}\right)$$

$$H_1 = 1 - 0.34\frac{a}{t} - 0.11\frac{a}{c}\left(\frac{a}{t}\right)$$

$$H_2 = 1 + G_1\left(\frac{a}{t}\right) + G_2\left(\frac{a}{t}\right)^2$$

$$G_1 = -1.22 - 0.12\left(\frac{a}{c}\right)$$

$$G_2 = 0.55 - 1.05\left(\frac{a}{c}\right)^{0.75} + 0.47\left(\frac{a}{c}\right)^{1.5}$$

Fig. 7. The evaluation of the stress intensity factor.

5. Results and Discussions

The threshold value for stress intensity factor, and subsequently the crack velocity, has been evaluated for a virtual crack presence in the possible locations over the whole pressure tube length.

Figure 8 shows the superposition of the values of K_{IH} obtained with the analytical model presented above and of the fit values, used for this parameter in coupling with CANTUP code. The fit law used has been a polynomial one:

$$K_{IH}(T) = 3.75 - 1.96\times10^{-3}\cdot T + 1.93\times10^{-5}\cdot T^2 \qquad (15)$$

the coefficient of determination R^2 being 0.999943 in the above equation, T is temperature in °K. The temperature range has been chosen to cover all the possible values for this parameter in the case of pressure tube. The temperature has been considered to vary over the tube length after a linear law, with a 266 ºC value at the inlet (left end, also considered as origin of *Ox* axis) and 312 ºC at the outlet (right end).

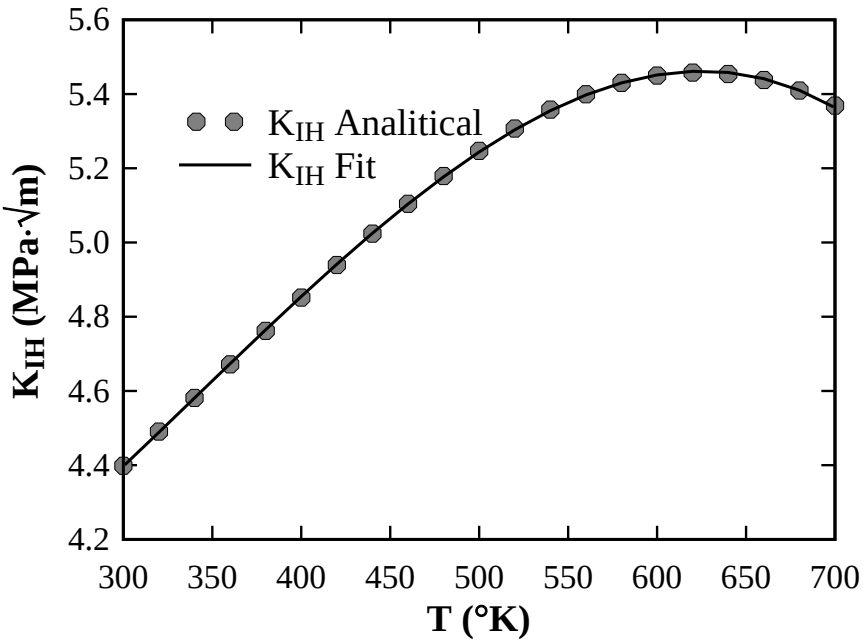

Fig. 8. Representation for initiation model and the fit law used in coupling with CANTUP.

The velocity of DHC phenomenon propagation is depicted with a 3D surface in Figure 9. It is shown the approximate independence of the velocity with the crack intensity factor in the plateau region, and the arrest temperature, which are dependent of stress intensity factor. Above the arrest temperature, the crack velocity drop down, fact experimentally confirmed.

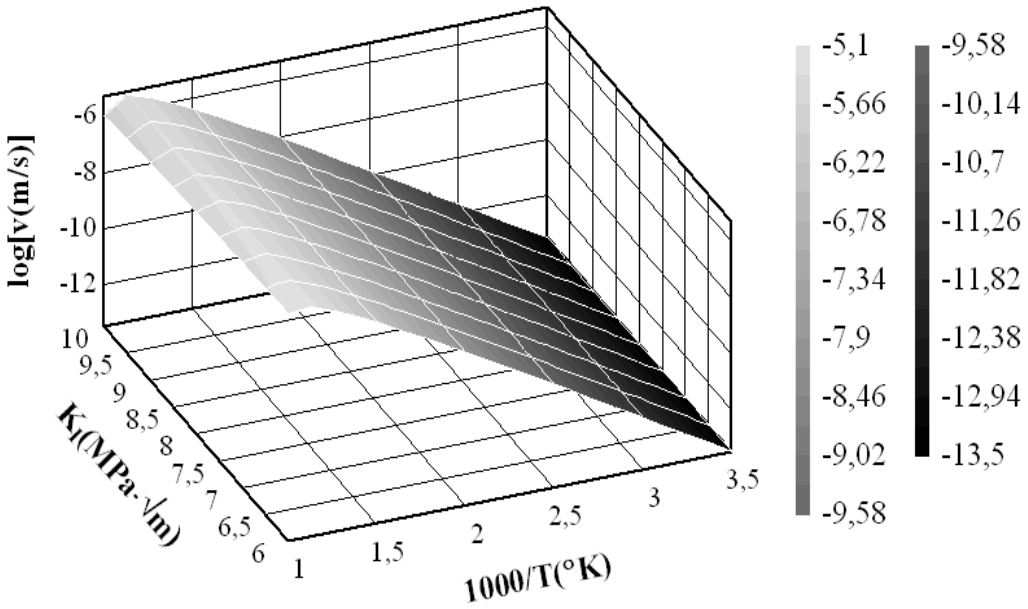

Fig. 9. The 3D representation of the DHC velocity over temperature and stress intensity factor.

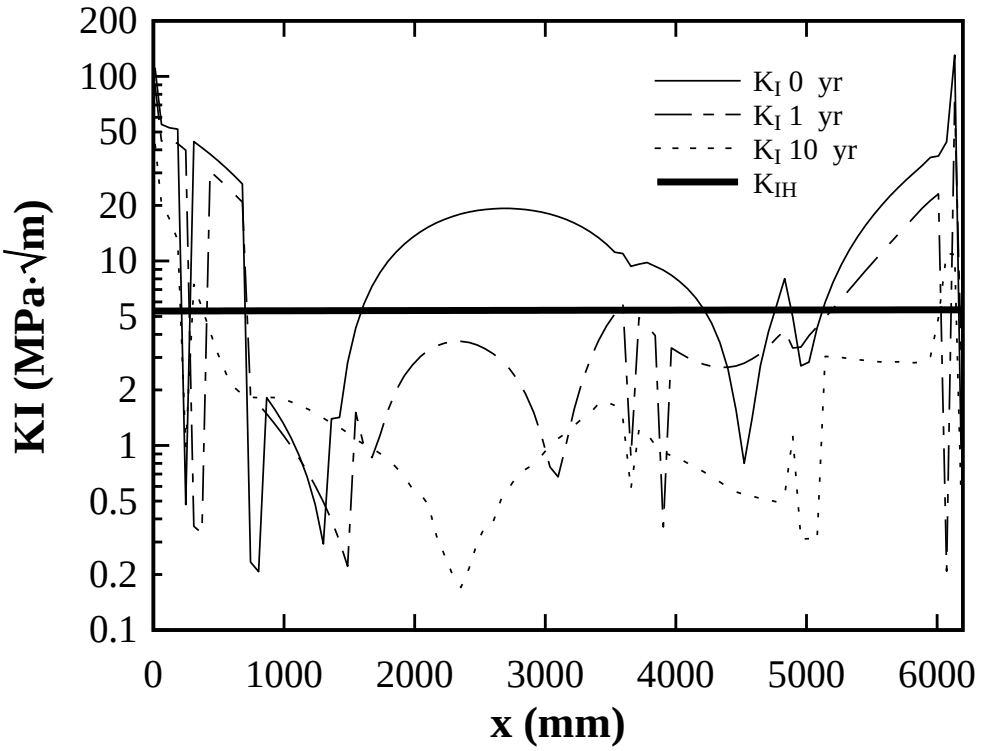

Fig. 10. The stress intensity factor evolution under creep irradiation conditions.

Figure 10 displays the evolution of the stress intensity factor, evaluated in creep conditions over an average of 10 years of service period under normal operating conditions.

It can be observed the relaxation tendency induced by the irradiation creep phenomenon. The decrease of the stress intensity factor it is more obvious in the middle zone of the equivalent bar of the pressure tube.

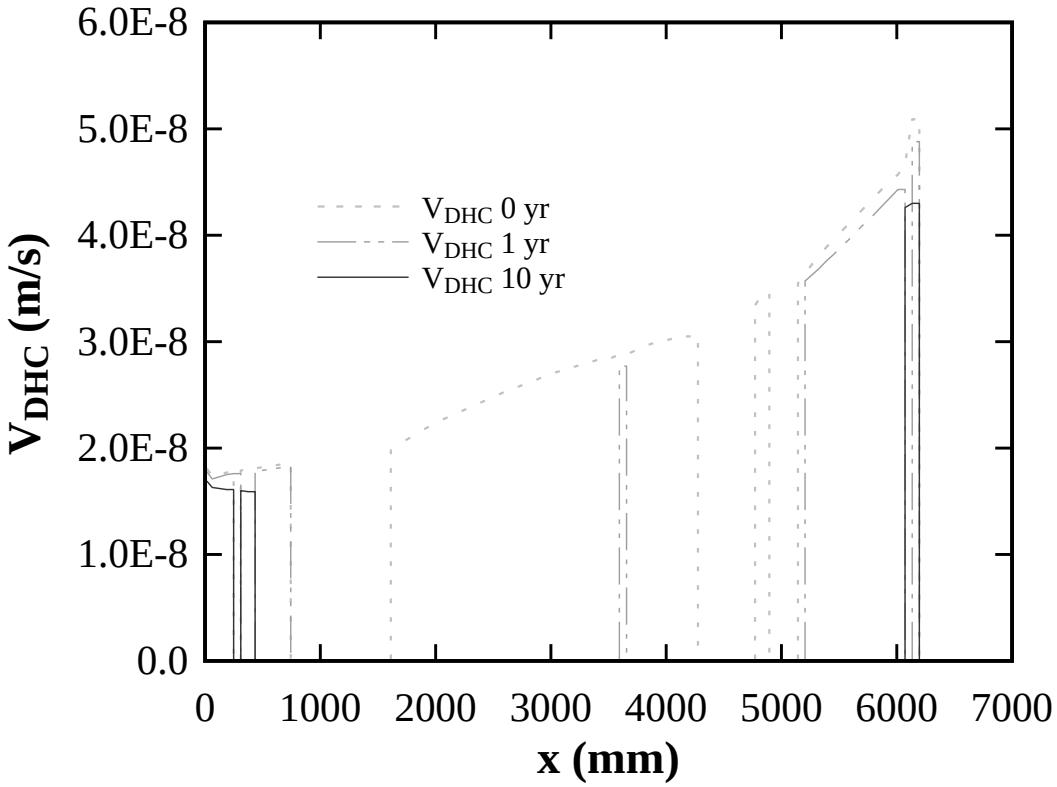

Fig. 11. The evolution of the DHC crack velocity obtained with CANTUP code coupled with DHC modeling.

In Figure 11 is depicted the DHC velocity obtained after the CANTUP FEM code and DHC modeling coupling. The velocity is evaluated along the whole pressure tube length. In the case that the evaluated stress intensity factor is under the threshold value, the velocity is null.

Over long time period, the regions of the pressure tube subjected to delayed hydride crack are restrained to the edges, fact which is experimentally confirmed [3]. Also, the velocity has a 10^{-8} order values (in m/s), which is also in agreement with experimental data obtained at Institute of Nuclear Research.

Conclusions

A presentation of the main aspects of DHC phenomenon has been made. The modeling of crack initiation and propagation has been implemented and verified against author's results.

The DHC modeling has been coupled with the FEM method based on CANTUP code, used at Institute for Nuclear Research in order to predict the long-time behavior of the CANDU pressure tube under normal operating conditions.

The code has been subsequently used to evaluate the long-time behavior of a presumptive crack, located in various places over the pressure tube length, with acceptable results. The values obtained for DHC velocity are similar with the experimental ones, and the most susceptible to DHC phenomenon zone of pressure tube are the ends.

R E F E R E N C E S

[1] W.L. Mudge, *Effect of hydrogen on the embrittlement of zirconium and zirconium alloys*, Symposium on Zirconium and Zirconium alloys, ASM, Metals Park, OH, (1953) 146–167.

[2] C.J. Simpson, C.E. Ells, *Delayed hydrogen embrittlement of Zr-2.5wt.%Nb*, J. Nucl. Mater., 52, (1974) 289–295.

[3] IAEA-TECDOC-1410, *Delayed hydride cracking in zirconium alloys in pressure tube nuclear reactors* - Final report of a coordinated research project 1998–2002, IAEA October, 2004.

[4] V. Radu, I. Popescu, *Dezvoltarea unui cod de calcul pentru analiza tensiunilor termoelastoplastice*, ICN Piteşti Rl 4638/1995.

[5] S. FLOREA, V. IONESCU, *Evaluarea probabilistică a stării de tensiuni şi deformaţii pentru componentele canalului de combustibil CANDU ca urmare a funcţionării îndelungate în reactor*, Rl 6130/2001.

[6] S. Florea, M. Pavelescu, *Assessments of long term mechanical behavior of CANDU fuel channel by means of PFEM analysis*, International Symposium on Nuclear Energy SIEN 2005, Nuclear Power - A New Challenge, Bucharest (Romania), 2005.

[7] C.E. Coleman *Cracking of Hydride-forming Metals and Alloys*, Comprehensive Structural Integrity, Elsevier, Eds. I. Milne, R.O. Ritchie and B. Karihaloo, 2003,Chapter 6.03, pp.103–161.

[8] Y.S. Kim, Y.G. Matvienko, Y.M. Cheong, S.S. Kim, S.C. Kwon, *A model of the threshold intensity factor, K_{IH}, for delayed hydride cracking of Zr-2.5Nb alloy*, J. Nuclear Materials 278 (2000) pp. 251 – 257.

[9] E.E. Gdoutos, *Fracture Mechanics, An Introduction, Second Edition,* Springer, 2005, p. 16.

[10] S. Florea, D. Ionescu, G. Horhoianu, M. Pavelescu, *Assessments of Delayed Hydride Cracking in Zr – 2.5% Nb Alloys*, International Symposium on Nuclear Energy SIEN 2007 Bucharest, Romania, October 14-19, 2007.

[11] R. Dutton, K. Nuttall, M.P. Puls, L.A. Simpson, *Mechanism of Hydrogen-Induced Delayed Hydride Cracking in Hydride Forming Materials*, Metall. Trans.A, 8A, (1977), 1553–1562.

[12] M.P. Puls, *Effects of Crack Tip Stress States and Hydride-matrix Interaction Stresses on Delayed Hydride Cracking*, Met. Trans. A, 21A, (1990), 2905–2917.

[13] T.L. Anderson, *Fracture Mechanics, Second Edition*, CRC Press, Boca Raton, New York, 1995, p. 627.

[14] S. Florea, M. Roth, *Modelarea fenomenului absorbţiei de hidrogen (DHC) la Zr-2.5% Nb*, RI 7199/2005.